

**Configuration and conductance evolution of benzene-dithiol molecular junctions under elongation**Nikolai Sergueev,<sup>1</sup> Leonidas Tsetseris,<sup>1,2</sup> Kalman Varga,<sup>1</sup> and Sokrates Pantelides<sup>1,3</sup><sup>1</sup>*Department of Physics and Astronomy, Vanderbilt University, Nashville, Tennessee 37235, USA*<sup>2</sup>*Department of Physics, National Technical University of Athens, GR-15780 Athens, Greece*<sup>3</sup>*Oak Ridge National Laboratory, Oak Ridge, Tennessee 37831, USA*

(Received 12 August 2010; published 30 August 2010)

Benzene-dithiol is a prototype molecular junction that exhibits a perplexing conductance behavior. Here we report density-functional total-energy and conductance calculations during a simulated elongation process, pulling the electrodes apart from an initial proximal distance, as in related experiments. We find that transformations between different elongation paths result in ranges of small and large conductances, fluctuations, and discontinuities. The obtained complex conformational and conductance evolution allows us to account for the experimental observations.

DOI: [10.1103/PhysRevB.82.073106](https://doi.org/10.1103/PhysRevB.82.073106)

PACS number(s): 81.07.Nb, 68.37.Ef, 72.10.-d, 73.63.-b

Potential nanoscale devices and fundamental questions about electron transport at the nanoscale have placed transport through individual molecules into the forefront of research interest. Different experimental techniques including the mechanically controlled break junction<sup>1–6</sup> and scanning tunneling microscopy<sup>7,8</sup> have been extensively used to study the electronic and structural properties of molecular devices. One of the most notable observations is that the conductance of many molecular tunneling junctions, especially those based on  $\pi$ -conjugated molecules, vary over a wide range.

Benzene-dithiol (BDT), a benzene ring with sulfur atoms attached at two ends to enable bonding to gold electrodes, has been studied extensively as a molecular junction. Experiments have reported BDT conductances ranging from the small  $0.0001G_0$  value of Reed *et al.*<sup>9</sup> to the  $0.1G_0$  data in the study of Tsutsui *et al.*<sup>10</sup> Furthermore, discrepancies have been reported with respect to conductance evolution under controlled increase in interelectrode separation distance. In particular, while in the study by Xiao *et al.*<sup>3</sup> repeated formation and breakup of BDT molecular junctions gave rise to conductance histograms with distinct conductance peaks at  $0.011G_0$ ,  $0.022G_0$ , and  $0.033G_0$ , similar studies by Ulrich *et al.*<sup>11</sup> and Martin *et al.*<sup>6</sup> found no preferred conductance peaks. A common feature in elongation experiments,<sup>3,6,11,12</sup> on the other hand, is the stepwise behavior of the conductance under elongation. These data suggest that there are more than one possible metastable molecular configurations and that elongation enforces abrupt transformations between these configurations, resulting in discontinuous changes in conductance.

The BDT junction has been studied extensively by theoretical calculations as well.<sup>13–19</sup> Reported values of the conductance also vary widely even for the equilibrium configuration<sup>20</sup> but the variation largely reflects differences in the underlying computational approaches. Beyond that, a number of theoretical studies have highlighted the significance of the structural and environmental parameters that influence the conductance measurements (molecular conformations, crystallographic orientation of the contacts, etc.).<sup>16–18,20–23</sup> Recent studies by Kamenetska *et al.*<sup>12</sup> and Paulsson *et al.*<sup>24</sup> simulated alkane-based molecular junctions as the electrodes are pulled apart and offered insights into the possible processes. In the latter study, finite-temperature

molecular-dynamics simulations showed variation in conductance traces for different elongation paths. The case of BDT molecular junctions, however, and the question, how the competition of different pulling sequences affects the evolution of conductance remain unresolved.

In this Brief Report, we report the results of density-functional total-energy and quantum-transport calculations of BDT molecular junctions under elongation, including a detailed study of the rupture process. We find that, unlike some alkane-based molecular junctions,<sup>12</sup> the BDT conductance is a strong function of the distance between the gold electrodes. In addition, two distinct bonding sites lead to very different conductance variations. Discontinuous jumps of  $G$ , reminiscent of the experimental steplike behavior, accompany transformations between different elongation paths. Transformations within the elongation paths also impact rapid changes in  $G$  in certain elongation range. Finally, we find that when the electrodes are brought closer, interelectrode tunneling is restored before they eventually crash onto each other.

We start modeling the BDT molecular junction by performing first-principles total-energy calculations to probe the stability of the BDT molecule between two metallic electrodes. We used the VASP numerical package<sup>25</sup> with a local-density approximation exchange-correlation functional,<sup>26</sup> projector-augmented wave potentials,<sup>27</sup> and plane waves as a basis set. The cutoff is set to 300 eV, and only the  $\Gamma$  point is used for  $k$ -point sampling. Energy barriers for switching between bonding configurations and for the break of the molecular junction at a particular elongation are calculated using the elastic band method<sup>28</sup> based on experience with other systems.<sup>29,30</sup> The periodic cell includes the BDT molecule and a Au slab up to six layers thick. The BDT molecule chemisorbs at several sites on the Au(111) surface. Bonding to the hollow site is energetically preferred over other high-symmetry structures, namely, the top and bridge configurations. The elongation paths we discuss below include hollow bonded geometries as intermediate structures. For this reason, even though differences in electrode surface morphology and relative interelectrode displacement give rise to several different elongation paths in practice, the atomic-scale details of the elongation sequences we have studied are representative and can account for key observed features.

The elongation of the BDT junction is of particular inter-

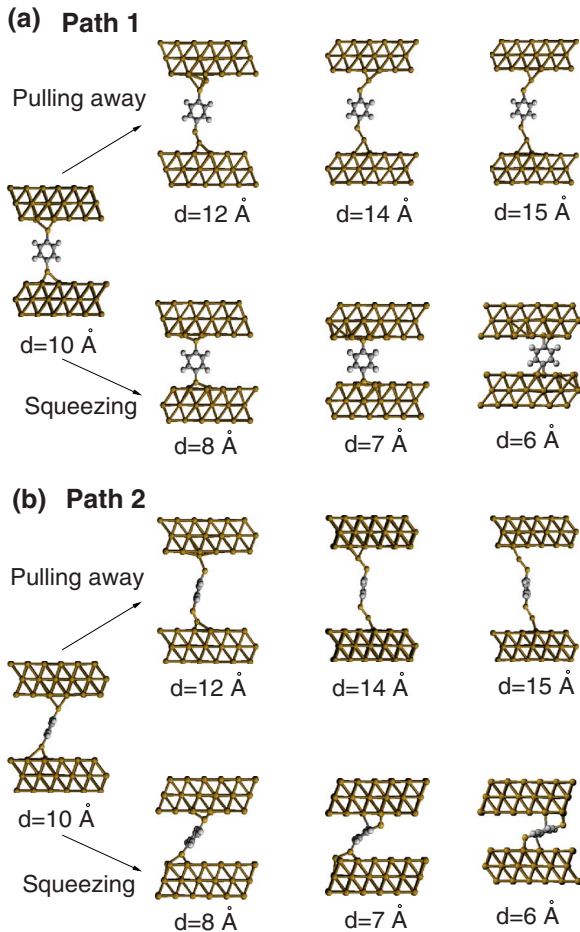


FIG. 1. (Color online) Equilibrium configurations of a Au-BDT-Au junction for various interelectrode separation gaps. Two elongation paths are shown as discussed in the text.

est in this work. Starting with the equilibrium configuration of the BDT junction for a certain interelectrode distance, we enlarge the dimension of the supercell in the direction of the junction by  $0.2 \text{ \AA}$  and then relax the structure to the new equilibrium. Because of the shallowness of the barriers between bonding configurations, stretching and/or squeezing leads back to bonding at the hollow site. When starting at the top bonding site, the molecule slid to hollow sites that are not directly opposite to each other, with the molecule tilted away from  $90^\circ$ . Thus we were able to get two distinct elongation paths, hereafter referred as Path 1 and Path 2. Several snapshots are shown in Fig. 1. The total energy versus contact separation is plotted for the two paths in Fig. 2(a).

Pushing the electrodes toward each other makes the energy first increase and then decrease drastically below the contact separation of  $6 \text{ \AA}$  for both adsorption configurations. When the contacts are very close to each other so that metal-metal bonds begin to form, the BDT junction crashes causing a dramatic decrease in the total energy. We find that the junction configuration with BDT in upright position bridging both electrodes is the energetically favorable configuration for the contact separations from  $7$  to  $10 \text{ \AA}$ . However, when the BDT junction breaks, the molecule tends to be in the flat configuration with the molecule parallel to the contact surface.

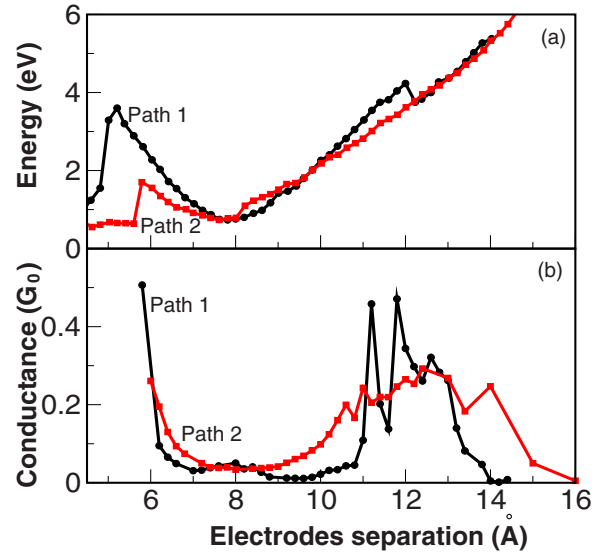


FIG. 2. (Color online) (a) Total energy of the Au-BDT-Au device versus the contact separation for the two paths. (b) Conductance versus electrodes separation for the two paths.

We examined more closely the stability of the molecular junction at elongations larger than  $10 \text{ \AA}$ , i.e., the regime when the rupture of the junction occurs. We found that such structures are metastable. An energy barrier is present for the bond to the exfoliated Au atom to break, with the Au atoms relaxing back to the surface and the molecule either remaining upright or folding back to a flat position on the surface of the other electrode. The value of the barrier for rupture is larger than  $1.3 \text{ eV}$  at  $9.7 \text{ \AA}$  and gets smaller at longer elongations, being only  $0.15 \text{ eV}$  at  $11.3 \text{ \AA}$ , suggesting that at finite temperatures the junctions would break spontaneously at elongations larger than  $10$ – $10.5 \text{ \AA}$ . The mechanical pull that is applied in the experiments described above can, in principle, cause breaks at even smaller separations.

Using the information from the total-energy calculations of the equilibrium configurations for the two elongation paths, we studied the variations in the transport properties of the junction. Specifically, for every atomic configuration along the elongation path we computed transport characteristics such as transmission probability coefficients and conductance using the “source-and-sink” method (see Ref. 19 for details). Figure 2(b) shows the conductance for the two paths at zero bias. We note that there are both similarities and differences in the conductance evolution of the two paths. First, at the separations less than  $6 \text{ \AA}$ , the conductance increases rapidly in both cases. This increase mainly results from direct tunneling from one contact to the other when the atomic orbitals of two electrodes start overlapping. Second, the conductance is low for elongations when the molecular junctions are stable, up to  $10 \text{ \AA}$ , and rises sharply in the metastable regime (elongations  $>10 \text{ \AA}$ ). Finally, at large electrode separations, when the metastable junction is about to break, the conductance decreases as the molecule starts to detach from one of the electrodes.

Figure 3 shows the distance between one of the BDT sulfur atoms and the nearest three surface gold atoms (Au1, Au2, and Au3) plotted versus contacts separation. As the

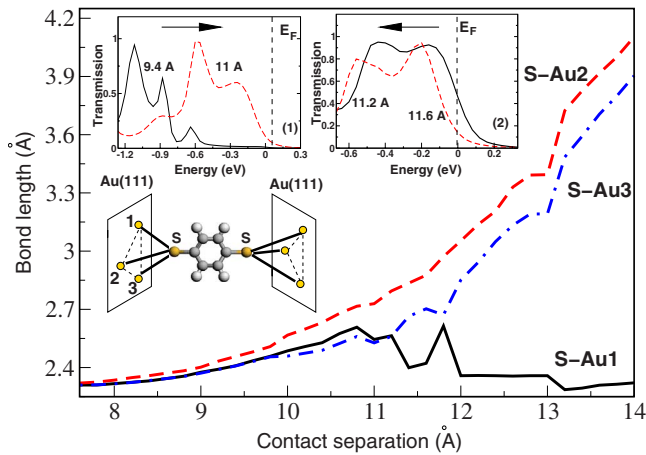


FIG. 3. (Color online) Distance between one of the BDT sulfur atoms and three nearest surface gold atoms. The BDT junction is elongated along the Path 1. The insets show the change in the transmission function when the S-Au1 bond length is increasing (9.4 and 11.0 Å, transmission peaks shift toward the Fermi energy) and when it is decreasing (11.2 and 11.6 Å, transmission peaks shift away from the Fermi energy).

junction is elongated along the Path 1, all three S-Au bond lengths stretch. After 10.75 Å, the S-Au2 and S-Au3 bond lengths continue increasing monotonically whereas the S-Au1 bond length gets shorter, gradually attaining its equilibrium value, suggesting that Au1 peels off the surface and creates a bridge as seen in Fig. 1. The variation in the S-Au1 bond length around 11–12 Å amounts to a “struggle” between the molecule and the electrode for possession of Au1. The slight oscillation in the S-Au1 bond length seen in Fig. 3 between 11 and 12 Å is in fact responsible for the rapid changes in conductance seen in Fig. 2(b), as illustrated in the insets of Fig. 3: in that short interval the peaks in the transmission function shift alternately to higher and lower energies, corresponding to alternate shorter and longer S-Au1 bond lengths.

We will now use the above theoretical results to analyze certain features of the experimental data of Refs. 3 and 11. The key data are conductance traces as a function of elongation. First, we note the theory predicts that truly stable BDT molecular junctions exist in the range of electrode separation of 7–10 Å (Fig. 4), which is consistent with the fact that in both experiments, in a single trace, a steplike behavior in the conductance occurs for elongations in the range 3–6 Å, after which, the molecular junction breaks.

The most notable feature of Fig. 4 is that conductance of BDT junction depends strongly on both the bonding configuration and the separation between the electrodes. This strong dependence, especially the fact that the conductance of a single BDT molecule *does not decrease monotonically* as a function of electrode separation rules out the possibility that the experimental conductance traces correspond to the junction capturing one molecule, then dropping it, then capturing another molecule and so on. The only possible explanation is that, in the initial step of the trace when the electrodes are brought to close proximity, several BDT molecules are captured and the observed conductance steps correspond to dropping one molecule at a time.

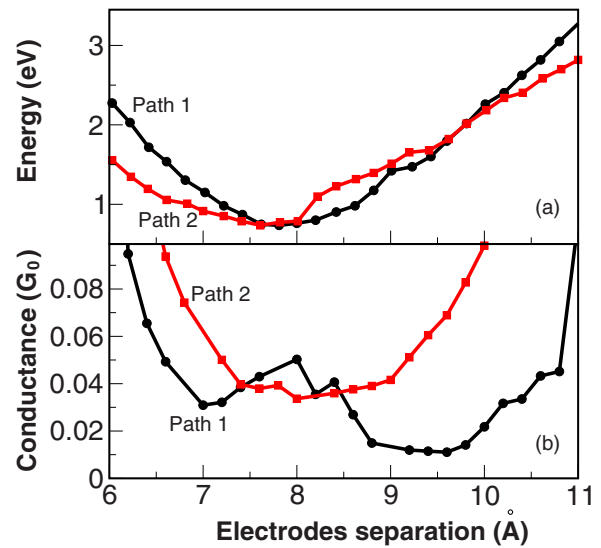


FIG. 4. (Color online) The zoom in of the calculated traces for the elongation range 6–11 Å: total energy (top) and conductance (bottom).

When the electrodes are in close proximity, BDT molecules are more likely to be captured as in Path 2, which is favored by as much as 1 eV. However, one or more molecules may be captured at longer effective electrode separations of 8–9.5 Å as in Path 1. At room temperature, even those that are initially bonded as in Path 2, may switch to Path 1 during elongation because the barrier for the switch is small. Thus, the molecules being dropped during the run are more likely, but not exclusively, those in Path 1. We note that from about 8.7–9.7 Å, the conductance of BDT molecules in Path 1 is relatively constant at slightly over  $0.01G_0$ . Thus, if the BDT molecules that are dropped during an experiment are primarily along Path 1 in the 8.7–9.7 Å stretch, distinct peaks in the conductance histogram would appear at multiples of about 0.01, as in the experiments of Ref. 3. If on the other hand, during the elongation process one ends up with a substantial number of molecules bonded as in Path 2, or possibly other paths, the conductance steps from dropping individual molecules would span a wide range from 0.01 to 0.1, perhaps more, without distinct peaks in the conductance histogram as in the data of Ref. 11.

As noted above, there are several factors that can affect the numbers and characteristics of the bonding geometries under elongation. Such factors include, for example, finite-temperature effects or the existence of different electrode morphologies. Though it is impractical for first-principles calculations to cover all the possibilities, our results provide guidelines to understand how these factors might control conductance traces. In particular, annealing may favor transformations between pulling paths, resulting thus in changes, some of them abrupt, in the conductance. On the other hand, rounder, sharper, or rougher tips might allow more contact geometries and larger variation in junction transport properties.

One of the interesting questions related to the elongation is the structural conformation of the BDT-electrodes interface as the BDT junction begins to rupture. The authors of

Refs. 3 and 11 report that the BDT junctions can be elongated by 3–6 Å and suggest a hypothesis that such stretching results from pulling the Au atoms of the electrodes rather than stretching the BDT molecule. As discussed in the previous paragraphs, the experimentally measured conductance steps are attributed to the elongation range of 7–11 Å. The results of the total-energy and conductance calculations suggest that pulling of gold atoms out of the contacts does occur when elongating the junction. However, it does not occur within the elongation range of 7–11 Å but rather when the contacts are even further retracted. This regime constitutes metastable bonding with a small energy barrier. It can potentially be reached experimentally at very low temperatures with very slow pulling of the electrodes. The results of the

calculations predict that, if elongation more than 11 Å were achieved, a sudden rise in the conductance would be observed.

In conclusion, we have presented a systematic first-principles study of BDT molecular junctions under an elongation process. Using density-functional total-energy and quantum-transport calculations, we investigated both the dynamical and transport properties of BDT molecular junctions. We find that the conductance of the BDT junction depends strongly on both the separation between the contacts and the trapping configuration of the BDT molecule. Finally, we find that the stretching of the junction results from pulling the gold atoms out of the electrodes accompanied by a sudden rise in the conductance.

- 
- <sup>1</sup>B. Xu and N. Tao, *Science* **301**, 1221 (2003).
  - <sup>2</sup>N. Tao, *J. Mater. Chem.* **15**, 3260 (2005).
  - <sup>3</sup>X. Xiao, B. Xu, and N. Tao, *Nano Lett.* **4**, 267 (2004).
  - <sup>4</sup>L. Venkataraman, J. Klare, I. Tam, C. Nuckolls, M. Hybertsen, and M. Steigerwald, *Nano Lett.* **6**, 458 (2006).
  - <sup>5</sup>L. Venkataraman, J. Klare, C. Nuckolls, M. Hybertsen, and M. Steigerwald, *Nature (London)* **442**, 904 (2006).
  - <sup>6</sup>C. Martin, D. Ding, H. van der Zant, and J. van Ruitenbeek, *New J. Phys.* **10**, 065008 (2008).
  - <sup>7</sup>M. Dorogi, J. Gomez, R. Osifchin, R. P. Andres, and R. Reifenberger, *Phys. Rev. B* **52**, 9071 (1995).
  - <sup>8</sup>R. Andres, T. Bein, M. Dorogi, S. Feng, J. Henderson, C. Kubiak, W. Mahoney, R. Osifchin, and R. Reifenberger, *Science* **272**, 1323 (1996).
  - <sup>9</sup>M. Reed, C. Zhou, C. Muller, T. Burgin, and J. Tour, *Science* **278**, 252 (1997).
  - <sup>10</sup>M. Tsutsui, Y. Teramae, S. Kurokawa, and A. Sakai, *Appl. Phys. Lett.* **89**, 163111 (2006).
  - <sup>11</sup>J. Ulrich, D. Esiril, W. Pontius, L. Venkataraman, D. Millar, and L. H. Doerr, *J. Phys. Chem.* **110**, 2462 (2006).
  - <sup>12</sup>M. Kamenetska, M. Koentopp, A. C. Whalley, Y. S. Park, M. L. Steigerwald, C. Nuckolls, M. S. Hybertsen, and L. Venkataraman, *Phys. Rev. Lett.* **102**, 126803 (2009).
  - <sup>13</sup>M. Di Venira, S. Pantelides, and N. Lang, *Appl. Phys. Lett.* **76**, 3448 (2000).
  - <sup>14</sup>M. Di Venira, S. T. Pantelides, and N. D. Lang, *Phys. Rev. Lett.* **84**, 979 (2000).
  - <sup>15</sup>Y. Xue, S. Datta, and M. Ratner, *J. Chem. Phys.* **115**, 4292 (2001).
  - <sup>16</sup>H. Basch and M. Ratner, *J. Chem. Phys.* **119**, 11926 (2003).
  - <sup>17</sup>A. M. Bratkovsky and P. E. Kornilovitch, *Phys. Rev. B* **67**, 115307 (2003).
  - <sup>18</sup>Z. Li and D. S. Kosov, *Phys. Rev. B* **76**, 035415 (2007).
  - <sup>19</sup>K. Varga and S. T. Pantelides, *Phys. Rev. Lett.* **98**, 076804 (2007).
  - <sup>20</sup>S. Lindsay and M. Ratner, *Adv. Mater.* **19**, 23 (2007).
  - <sup>21</sup>J. Nara, W. Geng, H. Kino, N. Kobayashi, and T. Ohno, *J. Chem. Phys.* **121**, 6485 (2004).
  - <sup>22</sup>Y. Xue and M. A. Ratner, *Phys. Rev. B* **68**, 115407 (2003).
  - <sup>23</sup>V. García-Suárez, T. Kostyrko, S. Bailey, C. Lambert, and B. Buřka, *Phys. Status Solidi B* **244**, 2443 (2007).
  - <sup>24</sup>M. Paulsson, C. Krag, T. Frederiksen, and M. Brandbyge, *Nano Lett.* **9**, 117 (2009).
  - <sup>25</sup>G. Kresse and D. Joubert, *Phys. Rev. B* **59**, 1758 (1999).
  - <sup>26</sup>J. P. Perdew and A. Zunger, *Phys. Rev. B* **23**, 5048 (1981).
  - <sup>27</sup>P. E. Blöchl, *Phys. Rev. B* **50**, 17953 (1994).
  - <sup>28</sup>G. Mills, H. Jonsson, and G. Schenter, *Surf. Sci.* **324**, 305 (1995).
  - <sup>29</sup>L. Tsetseris, N. Kalfagiannis, S. Logothetidis, and S. T. Pantelides, *Phys. Rev. Lett.* **99**, 125503 (2007).
  - <sup>30</sup>L. Tsetseris and S. T. Pantelides, *Acta Mater.* **56**, 2864 (2008).